ELM ion energies in the ASDEX Upgrade far scrape-off layer

M. Kočan[1], S. Y. Allan[2], S. Carpentier-Chouchana[3], S. Elmore[2], J. P. Gunn[4], A. Herrmann[1], A. Kirk[2], M. Kubič[4], H. W. Müller[1], R. A. Pitts[3], V. Rohde[1] and the ASDEX Upgrade Team

[1] *Max-Planck-Institut für Plasmaphysik, Bolzmannstr. 2, D-85748 Garching, Germany*
[2] *Culham Centre for Fusion Energy, Abingdon, OX14 3DB, United Kingdom*
[3] *ITER Organization, Route de Vinon, CS 90 046, 13067 Saint Paul Lez Durance Cedex, France*
[4] *CEA, IRFM, F-13108 Saint-Paul-lez-Durance, France*

1. Introduction. Type I ELMs carry a significant fraction of their energy ΔW_{ELM} across the scrape-off layer (SOL) and are the dominant source of the first wall thermal load and impurity sputtering. In ITER, ΔW_{ELM} will be considerably larger compared to present tokamaks and the ELM-wall interaction may be an issue for the first wall lifetime and impurity production.

New measurements of the ELM ion energies by a retarding field analyzer (RFA) in the ASDEX Upgrade (AUG) far SOL are presented. Type I and, for the first time, mitigated ELMs are captured by a RFA at different ΔW_{ELM} and the outer midplane separatrix distance Δr_{sep}. A fluid model of the ELM filament parallel transport [1] is employed to obtain the characteristic range of the ELM-averaged filament radial propagation speeds v_{r}.

2. Experimental setup. RFA measurements were obtained in lower single null divertor H-mode discharges with the representative magnetic equilibrium shown in Fig. 1. Edge plasma parameters of these discharges are compiled in Tab. 1. Type I ELMs were measured at a neutral beam heating power P_{NBI} = 2.5 MW. Mitigated ELMs, produced by new in-vessel magnetic perturbation (MP) coils [2], were measured at P_{NBI} = 5 MW with the mode number n = 2 resonant MPs with the coil current of 900 A. In all discharges $\mathbf{B}\times\nabla B$ points downwards, I_{p} = 1 MA, $q_{95} \approx 4.7$, $R \approx 1.67$ m. The separatrix parallel collisionality $\nu_{\mathrm{e}}^{*} \approx$ 2-4.

Set	$T_{i\,ped}$ [eV]	$T_{e\,ped}$ [eV]	$n_{e\,ped}$ [10^{19} m^{-3}]	ΔW_{ELM} [kJ]	$\Delta W'_{ELM}$ [%]
1	350	300	7.3	36±7	23
2	300	250	6.9-7.1	28±10	22
3	400	350	6.8-7.0	34±12	22
4	400	400	6.8-7.1	56±7	31
5	350	250	7.6-7.8	27±6	19
6*	450	350	7.6-7.8	2±5	1

Table 1. *From left to right: set index, ion and electron temperatures and plasma density at the pedestal top (~1.5 cm inside the separatrix), plasma energy lost per ELM (absolute and relative to the pedestal energy). * Mitigated ELMs.*

A bidirectional RFA is mounted on the horizontal scanning probe drive 31 cm above the outer midplane, Fig. 1. Each analyzer consists of semi-permeable grids and a collector, separated from the plasma by a thin plate in which a narrow slit is cut. A standard ion retarding voltage scheme is applied to both analyzers [3]. The slit plate measures the ion current density j_{sat}. A collector measures the current of ions (I_{c}) that have enough kinetic energy to overcome the positive bias voltage applied to one of the grids V_{g1}. j_{sat} and I_{c} are sampled at 2 MHz. In this paper we present the data measured by the analyzer connected magnetically to the outer divertor (Fig. 1) and viewing the outer midplane around which the ELM filaments are typically ejected into the SOL.

3. Experimental results. Fig. 1 shows the time traces of j_{sat} and I_{c} measured in similar Type I ELMs for different V_{g1}. Δr_{sep} = 35 mm. j_{sat} and I_{c} feature synchronized bursts lasting several tens of μs, separated by up to several hundred microseconds, interwoven with smaller spikes. The

same ELM filamentary structure was observed in other tokamaks (e.g. references in [1]). Qualitatively similar filamentary structure is observed in mitigated ELMs. The filaments measured by the RFA were found to be well correlated with the time traces recorded by the fast visible light camera viewing the probe head. We recall that only ions striking the RFA with energies exceeding eV_{g1} (in electron volts) can be measured by the collector. High ELM ion energies in the far SOL were observed earlier by a RFA in JET [4]. The ELM ion current to the collector $I_{c\ ELM}$ decreases with increasing V_{g1} and almost vanishes at V_{g1} = 325 V. I_c is absent between ELMs meaning that most background ions are repelled and do not contribute to $I_{c\ ELM}$.

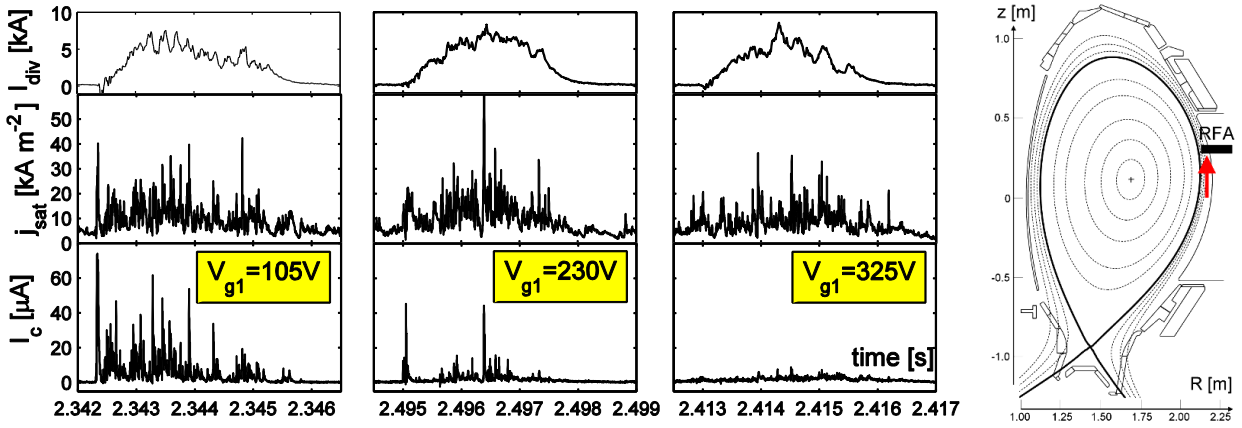

Figure 1. *RFA signals measured in similar Type I ELMs at Δr_{sep}=35 mm (set #1 from Tab. 1). The current to the inner divertor I_{div} serves as an ELM marker. V_{g1} is the ion repelling voltage applied at a given ELM. Right: Representative magnetic equilibrium of the database discharges with the AUG vessel structures and the RFA. Arrow indicates the poloidally-projected direction from which the RFA collects the data presented in this paper.*

The information about the radial expansion of ions in ELM filaments and their characteristic temperature can be estimated from the ELM-averaged ion current density $\langle j_{sat}\rangle$ and the collector current $\langle I_c\rangle$. j_{sat} values above 3σ threshold are selected from the time trace measured during an ELM. $\langle j_{sat}\rangle$ equals the mean of these data points. $\langle I_c\rangle$ equals the mean of the collector signal for the same time points. High ν_e^* makes it reasonable to expect that ELM ions have a drifting Maxwellian distribution of parallel speeds. Selecting from each discharge set ELMs measured at constant Δr_{sep}, the ELM ion temperature $T_{i\ ELM}$ can be obtained from the exponential fit to $\langle I_c\rangle$ plotted against V_{g1}, $\langle I_c\rangle \propto \exp(-V_{g1}/T_{i\ ELM})$, which is the standard RFA model. ELM ion current-voltage characteristics ($\langle I_c\rangle$ versus V_{g1}) are illustrated in Fig. 2.

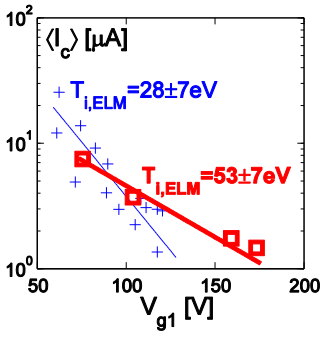

Figure 2. *The collector current averaged over an ELM, plotted against the ion repelling voltage. Each symbol corresponds to a single ELM. ELMs are measured at Δr_{sep} = 48 mm in the discharge set #5 (□) and #6 (+). The slope of the exponential fit to the measured data (full) is equal to the ELM ion temperature $T_{i\ ELM}$.*

Measurements of $T_{i\ ELM}$ are shown in Fig. 3. $T_{i\ ELM}$ decreases with increasing Δr_{sep} (e-folding length of $\lambda_{Ti} \approx 10$ mm) and increases rather strongly with ΔW_{ELM}. The same trend persists if ΔW_{ELM} is normalized to the total plasma or the pedestal energy. Smallest $T_{i\ ELM}$ is measured in mitigated ELMs. The decrease of $T_{i,ELM}$ with increasing Δr_{sep} is easily explained by the energy loss along the field lines to the solid surface as the ELM filaments propagate across the SOL. Strong dependence of $T_{i\ ELM}$ on ΔW_{ELM} might have two possible interpretations:

filaments of larger ELMs (i) are ejected into the SOL with higher initial temperatures and thus arrive hotter into the far SOL or (ii) they propagate faster radially and have less time to lose their energy along the field lines (or (iii) a combination of both). (i) would be surprising, given that hotter ELM filaments are also subject to stronger parallel energy loss because of larger sound speed c_s. A large variation of the initial ELM filament temperature would, therefore, result in relatively small changes in the far SOL $T_{i\,ELM}$. (ii) is addressed in what follows.

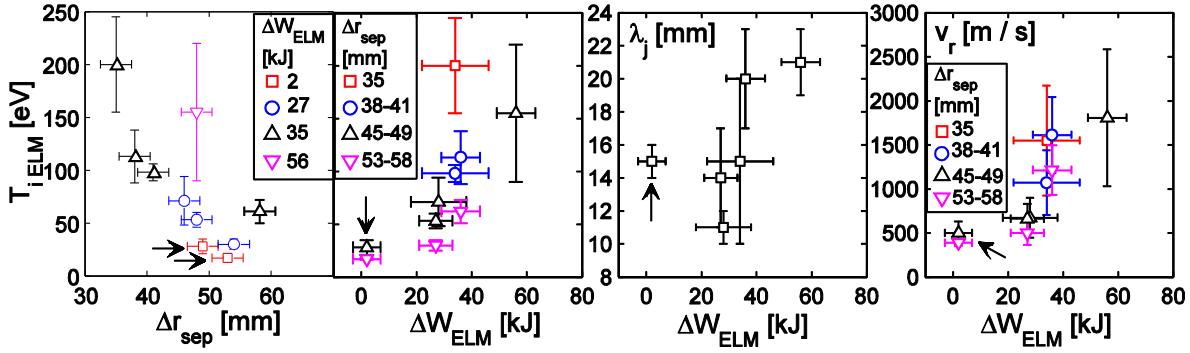

Figure 3. *From left to right: The ELM-averaged ion temperature plotted against the midplane separatrix distance as well as the energy lost per ELM, e-folding length of the ELM ion current density and the radial ELM-averaged filament propagation speed estimated from RFA measurements of $T_{i\,ELM}$ and λ_j. Arrows indicate mitigated ELMs.*

A balance between the characteristic parallel loss time and the perpendicular transport time is used to estimate from the RFA measurements the ELM-averaged filament radial propagation speed $v_r \approx \lambda_j c_s / L_{//}$ [5]. $c_s/L_{//}$ accounts for the parallel sink rate. c_s is approximated by $(eT_{i\,ELM}/m_i)^{1/2}$ assuming $T_{i\,ELM} > T_{e\,ELM}$. $T_{i\,ELM}$ and λ_j (the radial e-folding length of $\langle j_{sat} \rangle$) are taken from Fig. 3. Note that $T_{i\,ELM}$ values measured in similar ELMs at different Δr_{sep} correspond to a single λ_j. Since the filaments are connected to a solid surface at each end of the flux tube, $L_{//}$ equals one half of the harmonic mean of the length of the field lines between either side of the filament and the nearest surface. However, in the frame of a toroidally rotating filament, $L_{//}$ can vary in the far SOL due to toroidally discrete structures such as the limiters. This makes the evaluation of the "effective" $L_{//}$ cumbersome. In the far SOL of the present discharges, $L_{//}$ obtained from the field lines tracing at the outer midplane at a random toroidal location is at most a few meters. We assume $L_{//} \approx 1$ m, so that we might overestimate v_r. As seen from Fig. 3, v_r tends to increase with ΔW_{ELM} which (assuming that the same trend holds in the near SOL) would be consistent with (ii) and could explain the inverse scaling of the JET divertor ELM energy fraction [5] as well as increase of the JET limiter ELM loading with ΔW_{ELM} [6]. No radial variation of v_r is observed within the uncertainty of the measurements.

4. Modelling the ELM filament transport. A fluid model of the parallel ELM filament transport developed in [1] is used to reconcile the observations from Sec. 3. Once the initial filament temperatures and densities are specified, their time evolution due to parallel transport to the nearest surface is calculated. $T_{i\,ped}$ and $n_{e\,ped}$ for Tab. 1 determine the initial filament parameters (with $T_{e\,ped} = T_{i\,ped}$ for simplicity). Temporal and radial evolution of a filament is coupled through v_r, which is assumed to be radially constant. v_r is adjusted to bring modelled ELM filament ion temperature into exact agreement with the RFA measurements, as illustrated in Fig. 4. The error bar of v_r is obtained by matching the confidence interval of $T_{i\,ELM}$. $T_{i\,ELM} > T_{e\,ELM}$, a general trend, is because of the higher parallel conductivity of electrons compared to that of ions. $\lambda_{Ti} \approx$ 10-20 mm in the far SOL is in a good agreement with measured $\lambda_{Ti} \approx 10$ mm.

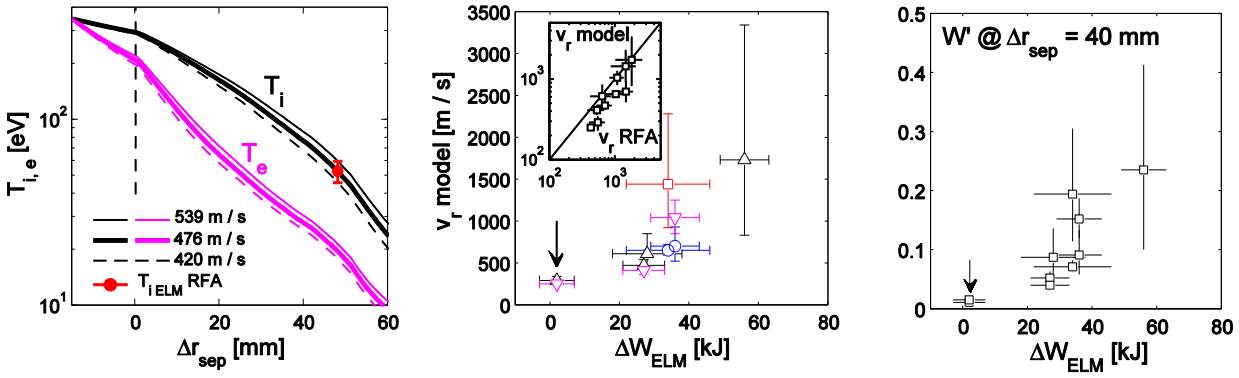

Figure 4. *Simulations results. Left: The ELM filament ion and electron temperatures as a function of the separatrix distance Δr_{sep}. The filament is launched from the pedestal top (Δr_{sep}= -1.5 mm, $T_{i\ ped}$ = $T_{e\ ped}$ = 350 eV, $n_{e\ ped}$ = 7.7·10^{19} m^{-3}). The radial ELM filament propagation speed v_r is adjusted to match $T_{i\ ELM}$ = 53±7 eV measured by the RFA at Δr_{sep} = 48 mm. Middle: v_r required to bring simulated $T_{i\ ELM}$ into exact agreement with the RFA measurements (Fig. 3). v_r is plotted against the energy lost per ELM ΔW_{ELM}. Δr_{sep} is color-coded as in Fig. 3. Inset panel compares v_r from the model with the RFA estimates from Sec. 3. Right: The filament stored energy at Δr_{sep} = 40 mm normalized to its initial value. Arrows indicate mitigated ELMs.*

The range of v_r from the simulations is plotted against ΔW_{ELM} in Fig. 4. The range of v_r as well the dependence on ΔW_{ELM} is very similar to RFA measurements in Fig. 3, suggesting that we have chosen reasonable $L_{//}$. For the reasons mentioned earlier, v_r obtained from the simulations is insensitive to the initial filament temperatures. v_r would vary at most by 11% if $T_{i\ ped}$ = $T_{e\ ped}$ = 350 eV were assumed in all simulations. Also shown in Fig. 4 is the filament stored energy W' at Δr_{sep} = 40 mm, normalized to its initial value at the pedestal top. W' is proportional to ΔW_{ELM}, which is a simple consequence of larger v_r required in the simulations to match $T_{i\ ELM}$ measured at higher ΔW_{ELM}. Filaments of the largest ELMs arrive at Δr_{sep} = 40 mm with up to 40% of their initial energy. Therefore, larger ELMs might be associated with smaller relative thermal loads to the divertor in exchange of larger first wall loading. This is consistent with the thermographic observations in JET [6,7]. W' in Fig. 4 agrees with an earlier energy balance study in AUG in which 15% of ΔW_{ELM} = 25 kJ was found on the outboard limiters in the Type I ELMy discharge with a separatrix-wall gap of 5 cm [8].

5. Summary. First systematic measurements of ion energies in Type I and mitigated ELMs were carried out in the far SOL of AUG using a RFA. The ELM-averaged ion temperatures $T_{i\ ELM}$ ≈ 20-200 eV, which corresponds to 5-50 % of the ion temperature at the pedestal top, were observed 35-60 mm outside the separatrix (i.e. 15-25 mm in front of the outboard limiters). $T_{i\ ELM}$ decreases with the separatrix distance with an e-folding length of ~10 mm. Lowest $T_{i\ ELM}$ was observed in mitigated ELMs. The increase of the energy lost per ELM is associated with the increase of $T_{i\ ELM}$ and the flattening of the ELM ion current density profile. This suggests that on average the filaments in larger ELMs might propagate faster across the SOL and thus deposit larger fraction of their energy on the first wall in exchange for smaller relative divertor loading.

Acknowledgements. In this work we used the script of the parallel loss model written by Dr. D. Moulton at JET.
References. [1] W. Fundamenski *et al.*, Plasma Phys. Control. Fusion **48** (2006) 109, [2] W. Suttrop *et al.*, Fusion Eng. & Design **84** (2009) 290. [3] M. Kočan *et al.*, Plasma Phys. Control. Fusion **53** (2011) 065002, [4] R. A. Pitts *et al.*, Nucl. Fusion **46** (2006) 82, [5] A. Kirk *et al.*, Plasma Phys. Control. Fusion **53** (2011) 035003, [6] T. Eich *et al.*, J. Nucl. Mater. **337-339** (2005) 669, [7] W. Fundamenski *et al.*, Proc. 22nd IAEA Fusion Energy Conf., Geneva, 2008, [8] A. Herrmann *et al.*, Plasma Phys. Control. Fusion **46** (2004) 971.